Radiology

Pulmonary Intravascular Lymphomatosis: Clinical, CT, and PET Findings, Correlation of CT and Pathologic Results, and Survival Outcome[1]

Min Jae Cha, MD
Kyung Soo Lee, MD
Hye Sun Hwang, MD
Tae Jung Kim, MD
Tae Sung Kim, MD
Byung-Tae Kim, MD
Young-Hyeh Ko, MD
Young Mog Shim, MD

Purpose: To describe clinical, computed tomographic (CT), and positron emission tomographic (PET) features, correlation of CT and pathologic results, and survival of patients with pulmonary intravascular lymphomatosis.

Materials and Methods: The institutional review board approved this retrospective study with waiver of patient consent. Forty-two patients with pulmonary intravascular lymphomatosis were identified, 11 (26%) of whom showed lung involvement. CT features were correlated with histopathologic results. Clinical and survival outcomes were compared between patients with and those without pulmonary involvement by adopting the χ^2, Student *t*, or Kaplan-Meier analysis with log-rank tests.

Results: At clinical presentation, all 11 patients showed B symptoms (systemic symptoms of fever, night sweats, and weight loss), 10 had respiratory and four had neurologic symptoms, and two had skin lesions. Patients received cyclophosphamide, doxorubicin, vincristine, and prednisone chemotherapy with (n = 5) or without (n = 6) rituximab, and seven (64%) patients died. Patients with lung involvement showed reduced overall and recurrence-free survival (median; 10.8 and 18.9 months, respectively) compared with those without lung involvement (median, 18.4 and 31.0 months, respectively) (P = .338 and .065, respectively). The most common CT abnormality was bilateral ground-glass opacity (GGO, n = 10), with increased fluorodeoxyglucose uptake at PET/CT (seven of seven patients). GGO correlated histopathologically with the expanded alveolar septal vasculatures and perivascular spaces filled with neoplastic lymphoid cells.

Conclusion: Pulmonary intravascular lymphomatosis appeared as bilateral GGO on CT images, with increased fluorodeoxyglucose uptake on PET/CT images. GGO on CT images correlated with the area of expanded alveolar septae because of distended vessels filled with neoplastic lymphoid cells.

Online supplemental material is available for this article.

[1] From the Department of Radiology and Center for Imaging Science (M.J.C., K.S.L., H.S.H., T.J.K., T.S.K.), Department of Nuclear Medicine (B.T.K.), Department of Pathology (Y.H.K.), and Department of Thoracic Surgery (Y.M.S.), Samsung Medical Center, Sungkyunkwan University School of Medicine, 50 Ilwon-Dong, Kangnam-Ku, Seoul 135-710, Korea. Received August 7, 2015; revision requested September 29; revision received October 27; accepted December 15; final version accepted January 7, 2016. **Address correspondence to** K.S.L. (e-mail: *kyungs.lee@samsung.com*).

Intravascular lymphomatosis (IVL), also known as malignant endotheliomatosis or angiotropic large-cell lymphoma, is a rare and distinctive form of malignant lymphoma characterized by the proliferation of neoplastic lymphoid cells, mostly of B-cell origin, in the vascular lumina (1,2). The disease can affect vessels in any organ. However, authors have reported (3–5) that patients who received a diagnosis of IVL in Western countries display a propensity for central nervous system and skin involvement, while those diagnosed in Asian countries are more likely to show hemophagocytic syndrome, bone marrow involvement, fever, hepatosplenomegaly, and thrombocytopenia.

The clinical features of IVL are nonspecific, but IVL most commonly manifests as fever of unknown origin, weight loss, night sweats, dementia, and cutaneous nodules or plaques (6). With vascular occlusion of various organs and attendant diverse and confusing clinical presentations, the diagnosis of IVL is usually deferred. IVL has been confused with other possible conditions including vasculitis, dementia, or infarction, occult neoplasm, and infection. When the lungs are involved, patients experience shortness of breath, hypoxemia, and, rarely, pulmonary hypertension, and the disease may simulate various lung diseases, particularly diffuse interstitial lung disease or a subacute or chronic infectious condition (6,7). Moreover, due to the rarity of this condition, ready diagnosis of the disease is difficult, and lung lesions in patients with IVL are often detected at autopsy (8).

To date, there have been several reports (8–10) about the radiologic findings of lung IVLs. Although the main computed tomographic (CT) finding of lung IVLs is diffuse ground-glass opacity (GGO), the disease also may demonstrate subpleural patchy areas of consolidation and reticulonodular lesions. These CT manifestations of IVL are nonspecific and can be seen in patients with diverse diseases, which may cause delayed diagnosis of this rapidly progressive and diffuse vascular tumorous condition. Consequently, chest physicians and radiologists should recognize this unusual vascular lymphoma as a possibility in the differential diagnosis of diffuse lung diseases. Thus, the purpose of our study was to describe clinical, CT, and positron emission tomographic (PET) features, correlation of CT and pathologic results, and survival outcomes in patients with pulmonary IVL.

Advances in Knowledge

- At presentation, 11 of 11 (100%) patients with pulmonary intravascular lymphomatosis (IVL) demonstrated B symptoms (systemic symptoms of fever, night sweats, and weight loss), 10 (91%) had respiratory symptoms, 10 (91%) had elevated serum lactate dehydrogenase, seven (64%) had hypoalbuminemia, five (45%) had pulmonary hypertension, and four (36%) had a decrease in diffusion capacity of the lung.
- The most common abnormality seen on CT images in patients with pulmonary IVL was bilateral ground-glass opacity in 10 of 11 (91%) patients, and the area correlated histopathologically with the area of expanded alveolar septae and perivascular spaces because of distended septal capillaries, venules, and arterioles filled with neoplastic lymphoid cells.
- Patients with lung involvement of IVL showed reduced overall and recurrence-free survival compared with those without lung involvement, although it was not statistically significant ($P = .338$ and .065, respectively).

Implications for Patient Care

- Persistent ground-glass opacity with an enlarged pulmonary trunk in patients with B symptoms (fever, night sweats, and weight loss), respiratory symptoms, elevated serum lactate dehydrogenase, and hypoalbuminemia may suggest the diagnosis of pulmonary IVL.
- Because prognoses are relatively poor in patients with pulmonary IVL, recognition of this unusual vascular lymphoma clinically and radiologically may help in planning early invasive diagnostic workup.

Materials and Methods

Our institutional review board approved this retrospective study, and the requirement for patient consent for use of clinical data was waived.

Study Patients

A review of the electronic medical records allowed us to find all the patients with histopathologically proven IVL at our institution from November 1994 through May 2015. We searched the whole electronic medical record database for patients who had pathologic diagnoses containing the terms "intravascular," with "lymphomatosis" or "lymphoma," and consequently, we identified a total of 42 cases of IVL in 42 consecutive patients; the sites of involvement in these patients were bone marrow in 20 (48%), lymph nodes in 16 (38%), central nervous system in 13

Published online before print
10.1148/radiol.2016151706 **Content codes:** CH CT

Radiology 2016; 280:602–610

Abbreviations:
CHOP = cyclophosphamide, doxorubicin, vincristine, and prednisone
FDG = fluorodeoxyglucose
GGO = ground-glass opacity
IVL = intravascular lymphomatosis

Author contributions:
Guarantors of integrity of entire study, K.S.L., Y.M.S.; study concepts/study design or data acquisition or data analysis/interpretation, all authors; manuscript drafting or manuscript revision for important intellectual content, all authors; approval of final version of submitted manuscript, all authors; agrees to ensure any questions related to the work are appropriately resolved, all authors; literature research, M.J.C., K.S.L., H.S.H., T.J.K.; clinical studies, K.S.L., T.J.K., T.S.K., B.T.K., Y.H.K., Y.M.S.; experimental studies, Y.H.K.; statistical analysis, M.J.C., K.S.L.; and manuscript editing, K.S.L.

Conflicts of interest are listed at the end of this article.

(31%), liver and spleen in nine (21%), skin in nine (21%), kidney in five (12%), gastrointestinal tract in four (10%), adrenal gland in four (10%), and urinary bladder in two (5%) patients. Staging with the Ann Arbor classification system showed 37 patients with stage 4, one with stage 3, two with stage 2, and two patients with stage 1 disease.

The lungs were involved in 11 (26%) patients, and this was confirmed pathologically (n = 9) or clinically (n = 2). One patient was included whose imaging features were published in our previous study (9). Nine patients who had pathologic confirmation of IVL on the basis of lung biopsy results also showed involvement of other organs such as bone marrow (n = 2), liver (n = 1), lymph nodes (n = 1), appendix (n = 1), and paranasal sinus (n = 1). The clinical diagnosis of lung IVL was established with the fulfillment of three prerequisite conditions: pathologic confirmation of IVL from any organs other than the lungs, persistent or progressive pulmonary lesions during the follow-up period, and therapeutic response of lung lesions to IVL chemotherapy. In one patient, the histologic diagnosis of IVL was made on the basis of bone marrow and liver biopsy results and showed persistent, diffuse GGO on CT images throughout the follow-up period of 1 month and complete resolution of the lesions after chemotherapy. In the other case, the histologic confirmation was made on the basis of bone marrow biopsy results and demonstrated progression of GGO lesions on CT images throughout the follow-up period of 13 months and response to chemotherapy. The diagnosis was made on the basis of the multidisciplinary approach of clinicians, radiologists, and pathologists.

Clinical Assessment

The clinical information was available from patient medical records. We screened the data including sex; symptoms; age at diagnosis; premorbid conditions; affected organs; histopathologic results; laboratory values including hemoglobin level, platelet count, and serum albumin and lactate dehydrogenase levels; results of pulmonary function tests and echocardiography; and response to treatment. Survival and the presence of disease recurrence were also assessed by reviewing medical records and data from the Korean National Statistical Office. Overall survival was defined as the interval from the time of diagnosis to the date of death or final follow-up visit (11). Recurrence-free survival was defined as the interval from the time of diagnosis to the point of any definite clinical or pathologic evidence of disease recurrence or the last evaluation (12). Recurrence-free survival was available only for the patients who completed chemotherapy, because those who did not complete chemotherapy showed progression without treatment response and did not undergo the requisite follow-up study.

The 11 patients (mean age, 53 years; range, 30–71 years) with confirmation of lung IVL included three men (mean age, 54 years; range, 41–69 years) and eight women (mean age, 53 years; range, 30–71 years). The Fisher exact test results showed that age did not differ significantly between male and female patients (P = .93). Four patients had a premorbid condition such as hypertension (n = 2), seropositive rheumatoid arthritis (n = 2), or hypothyroidism (n = 1). B symptoms (systemic symptoms of fever, night sweats, and weight loss) were identified in all (100%) patients. Respiratory symptoms such as cough, sputum, and dyspnea were present in 10 (91%) patients. Neurologic symptoms including severe headache and motor and sensory problems were present in four (36%) patients, and skin lesions were detected in two (18%) patients. In two (18%) patients, the lungs were the sole organ of IVL involvement (Table 1).

Table 1

Clinical and Laboratory Findings of 11 Patients with Lung IVL

Variable	Data
Age (y)	54 (41–71)*
B symptoms	11 (100)
Abnormality	
B cell	11 (100)
T cell/natural killer cell	0 (0)
Sites of involvement, along with the lung	
Bone marrow	5 (45)
Tumor cell infiltration	4 (36)
Hemophagocytic histiocytosis	4 (36)
Liver and spleen	5 (45)
Central nervous system	4 (36)
Lymph nodes	5 (45)
Gastrointestinal tract	2 (18)
Skin	2 (18)
Kidney	2 (18)
Laboratory findings	
Anemia, hemoglobin < 120 g/L	5 (45)
Thrombocytopenia, $< 150 \times 10^9$/L	4 (36)
Serum lactate dehydrogenase, elevated	10 (91)
Hypoalbuminemia, < 36 g/L	7 (64)

Note.—Unless otherwise indicated, data are number, of patients with percentages in parentheses. B symptoms = fever, night sweat, and weight loss.

* Data are medians, with the range in parentheses.

Image Acquisition and Interpretation

Serial CT studies were available for all 11 patients who were the targets of this retrospective review. CT studies were performed by using various helical CT scanners (Hi Speed Advantage, Light Speed 16, Light Speed Ultra, Light Speed VCT, and Discovery CT750 HD; GE Healthcare, Chalfont St Giles, England; Brilliance 40; Philips, Best, the Netherlands). CT scans (amperage, 114–210 mA; voltage, 120 kVp; beam width, 10–20 mm; beam pitch, 1.375–1.5) were performed from lung apices to the level of the middle portion of both kidneys. An intravenous contrast medium, iomeprol (300 mg of iodine per milliliter, Iomeron 300; Bracco; Milan, Italy), was injected in six patients at 1.5 mL/kg of body weight at an infusion rate of 3 mL/sec by using a power injector (MCT Plus; Medrad, Pittsburgh, Pa). The imaging data were reconstructed with a section thickness of 2.5–5.0 mm by using a bone algorithm. The reconstructed images were then interfaced directly into a picture archiving and communications system (Centricity 3.0; GE Healthcare, Mt Prospect, Ill).

Two chest radiologists (M.J.C. and K.S.L., with 5 and 30 years of experience in chest imaging interpretation, respectively) assessed chest CT images together, and decisions on CT findings were reached in consensus. On CT images, the patterns of parenchymal abnormalities were subdivided into areas of GGO, consolidation, nodules, and interlobular septal thickening (13). The presence of pleural effusion, pericardial effusion, and lymphadenopathy was also evaluated (14). Regarding the anatomic location, parenchymal abnormalities were classified as central, peripheral, or mixed distribution on the axial plane and upper lung zone–predominant, lower lung zone–predominant, or random distribution on the longitudinal plane (15). Laterality of the lesions also was recorded. In addition, readers measured the widest short-axis diameter of the main pulmonary artery on axial sections at the level of the bifurcation for the evaluation of pulmonary hypertension (16). The improvement or progression of CT features such as parenchymal abnormality, pleural or pericardial effusion, lymphadenopathy, and enlargement of the pulmonary trunk was determined on the basis of follow-up CT images, which were obtained during or after the treatment.

Seven of 11 patients also underwent fluorine 18 fluorodeoxyglucose (FDG) PET/CT. PET images were reviewed by an experienced nuclear medicine physician (B.T.K., with 30 years of experience in PET/CT interpretation). Nine of 11 patients underwent transthoracic echocardiography (Vivid 7; GE Medical Systems, Milwaukee, Wis) performed by experienced sonographers. All measurements were made according to the recommendations of the American Society of Echocardiography.

Pathologic Analysis

One experienced pathologist (Y.H.K., with 32 years of experience in histopathologic interpretation) interpreted all tissue specimens, and diagnoses were made according to World Health Organization classification. In nine patients with pathologic confirmation of pulmonary IVL, the specimens were obtained by means of video-assisted thoracoscopic surgery (n = 6), transbronchial lung biopsy (n = 2), or open surgical lung biopsy (n = 1). The mean time interval between CT examinations and pathologic diagnoses was 6 days (range, 2–56 days). Parenchymal abnormalities on CT images were correlated with the microscopic findings, and two radiologists (M.J.C. and K.S.L.) and a pathologist (Y.H.K.) made decisions on correlation in consensus.

Statistical Analysis

Differences in demographic and survival outcome data of the patients who showed lung involvement of IVL (pulmonary IVL group) and those who did not (nonpulmonary IVL group) were assessed by using the χ^2 test, the Fisher exact test, or the Student t test. Recurrence-free survival and overall survival were estimated by using the Kaplan-Meier method, and the log-rank test was used to evaluate the differences among the subgroups. Statistical analyses were performed with software (SPSS version 19.0; SPSS, Chicago, Ill). A P value of less than .05 was considered to indicate a significant difference.

Results

Clinical Features

All cases were of B-cell lineage, and were thus proven to be intravascular large B-cell lymphoma. Eight patients underwent pulmonary function tests. The results of flow-metric evaluation showed only one mild obstructive pattern, whereas the remaining seven patients demonstrated normal function. However, all four patients who were evaluated for diffusion capacity of the lung showed a decrease in diffusion capacity (range, 38.3%–76% of the predicted value). Of nine patients who underwent echocardiography, five showed a mild-to-moderate degree of pulmonary hypertension; in these five patients, four showed an enlarged main pulmonary artery compared with the accompanying ascending aorta at CT (Fig 1).

Image Findings

Patterns and distribution of CT findings are summarized in Table 2. The most common pattern of parenchymal abnormality was bilateral GGO (n = 10) (Figs 1, 2). In the background GGO, nodules were seen in five patients (Figs 1, 2), and consolidation was noted in four patients. Interlobular septal thickening and peribronchovascular interstitial thickening were noted in four and two patients, respectively. Lymphadenopathy was seen in two patients. Pleural effusion and pericardial effusion also were seen in four patients each. As shown in Figure 3, one patient showed distinctive CT findings of enlarged peripheral branching or tubular structures, which might have represented dilated vasculature or bronchiolar lesions. The abnormalities on CT images showed significant improvement in the eight patients who finished chemotherapy as planned. The parenchymal lesions predominantly involved the peripheral lungs rather than the central lungs in five patients. Regarding longitudinal plane involvement, upper lung zone predominance was noted in five patients, whereas the lesions showed random distribution in six patients. At FDG PET performed in seven patients, elevated FDG uptake was seen at the corresponding areas of abnormality on CT images in all seven patients (Figs 2, 3). The mean maximum standardized uptake value was 7.4 (range, 5.1–10.8).

Correlation of CT and Pathologic Results

As demonstrated in Figures 1 and 2 and Figure E1 (online), the area of GGO on CT images correlated histopathologically with the area of expanded alveolar septa and perivascular spaces attributed to distended septal capillaries, venules, and arterioles filled with neoplastic lymphoid cells. The alveolar congestion or hemorrhage was not obvious. Since atypical lymphoid cells were mainly located in the vessels, the interlobular septal thickening was not prominent on CT images (Figs 1, 2). The interlobular septal prominences were noted in four patients, and most of them were secondary to venous congestion rather than

Table 2

Patterns and Distribution of CT findings of Pulmonary IVL

CT findings	Data
Parenchymal abnormalities	
GGO	10 (91)
With consolidation	4 (36)
With nodules	5 (45)
With interlobular septal thickening	4 (36)
With peribronchovascular thickening	2 (18)
Nodules only	1 (9)
Associated findings	
Pleural effusion	4 (36)
Pericardial effusion	4 (36)
Lymphadenopathy	2 (18)
Distribution	
Axial plane	
Peripheral	5 (45)
Central	0 (0)
Random	6 (55)
Coronal plane	
Upper lung zone predominant	5 (45)
Lower lung zone predominant	0 (0)
Random	6 (55)

Note.—Data are number of patients, with percentage in parentheses.

Figure 1

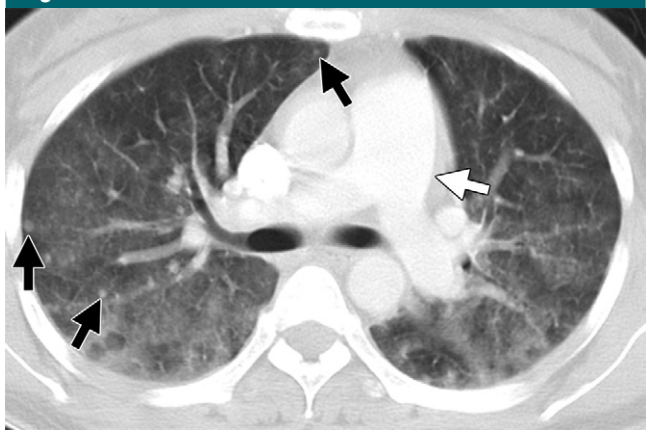

Figure 1: Axial (section thickness, 5.0 mm) CT image obtained at level of right upper lobar bronchus shows diffuse GGO lesions containing multiple small nodules (black arrows) in both lungs. Main pulmonary artery (white arrow) is enlarged and larger than ascending aorta, measuring 32 mm in diameter. Surgical lung biopsy results confirmed diagnosis of pulmonary IVL (Fig E2 [online]).

lymphatic involvement of lymphoma itself. Nodules, which were noted in five patients, formed mostly because of vascular filling, perivascular extension of atypical lymphoid cells, and associated perivascular fibrosis and inflammation. As for consolidation, alveolar filling with associated hemorrhage, flooded tumor cells, and interstitial fibrosis or inflammation accounted for the parenchymal opacity. The enlarged peripheral branching or tubular structures in Figure 3 represented dilated peripheral vessels (mostly venules) associated with the obstruction of blood flow due to neoplastic cells packing the small vessels. The lesions completely resolved after chemotherapy.

Survival Comparisons between Pulmonary and Nonpulmonary Groups

Table 3 demonstrates the results of comparison between patients who exhibited lung involvement of IVL and those who did not. Of the 11 patients with pulmonary IVL, six were treated with cyclophosphamide, doxorubicin, vincristine, and prednisone (CHOP) and five patients received the same four medications plus rituximab chemotherapy. Eight patients finished six or seven cycles of CHOP or CHOP and rituximab chemotherapy. Among 31 patients with IVL without lung involvement, 21 completed CHOP (n = 2) or CHOP with rituximab (n = 19) chemotherapy as planned.

Seven of 11 patients with pulmonary IVL eventually died, and the median overall survival time was 10.8 months (range, 0.7–44.8 months). Median survival was 8.6 months (range, 0.7–34.0 months) in seven patients with a lethal clinical course, whereas the median follow-up duration was 33.2 months (range, 1.1–51.2 months) in four survivors. Regarding the nonpulmonary IVL group, 12 patients died, and the median survival was 18.4 months (0.3–119.2 months).

All patients who received planned chemotherapy achieved complete remission at follow-up evaluation, except one patient in the nonpulmonary IVL group. Of the eight patients with pulmonary IVL, disease recurred in five. The median recurrence-free survival was 18.9 months (range, 4.8–44.8 months), whereas it was 5.6 months (range, 4.8–30.8 months) in patients with recurrent disease. Only five of the 21 patients with IVL without pulmonary involvement showed disease recurrence, and the median recurrence-free survival was 31.0 months (range, 6.9–119.2 months). Although it was not statistically significant, patients with lung involvement of IVL showed reduced recurrence-free survival rates compared with those without lung involvement (P = .065). The overall survival rate was not significantly different, either (P = .110). However, patients with lung involvement of IVL consistently showed a tendency toward poor overall survival, as demonstrated on survival curves in Figure E1 (online).

Discussion

The results of our study showed that pulmonary IVLs, all proven to be intravascular large B-cell lymphomas, manifested mostly as diffuse bilateral GGO on CT images. Other parenchymal abnormalities such as consolidation and nodules may accompany GGO. However, the rates of interlobular septal thickening, peribronchovascular

Figure 2

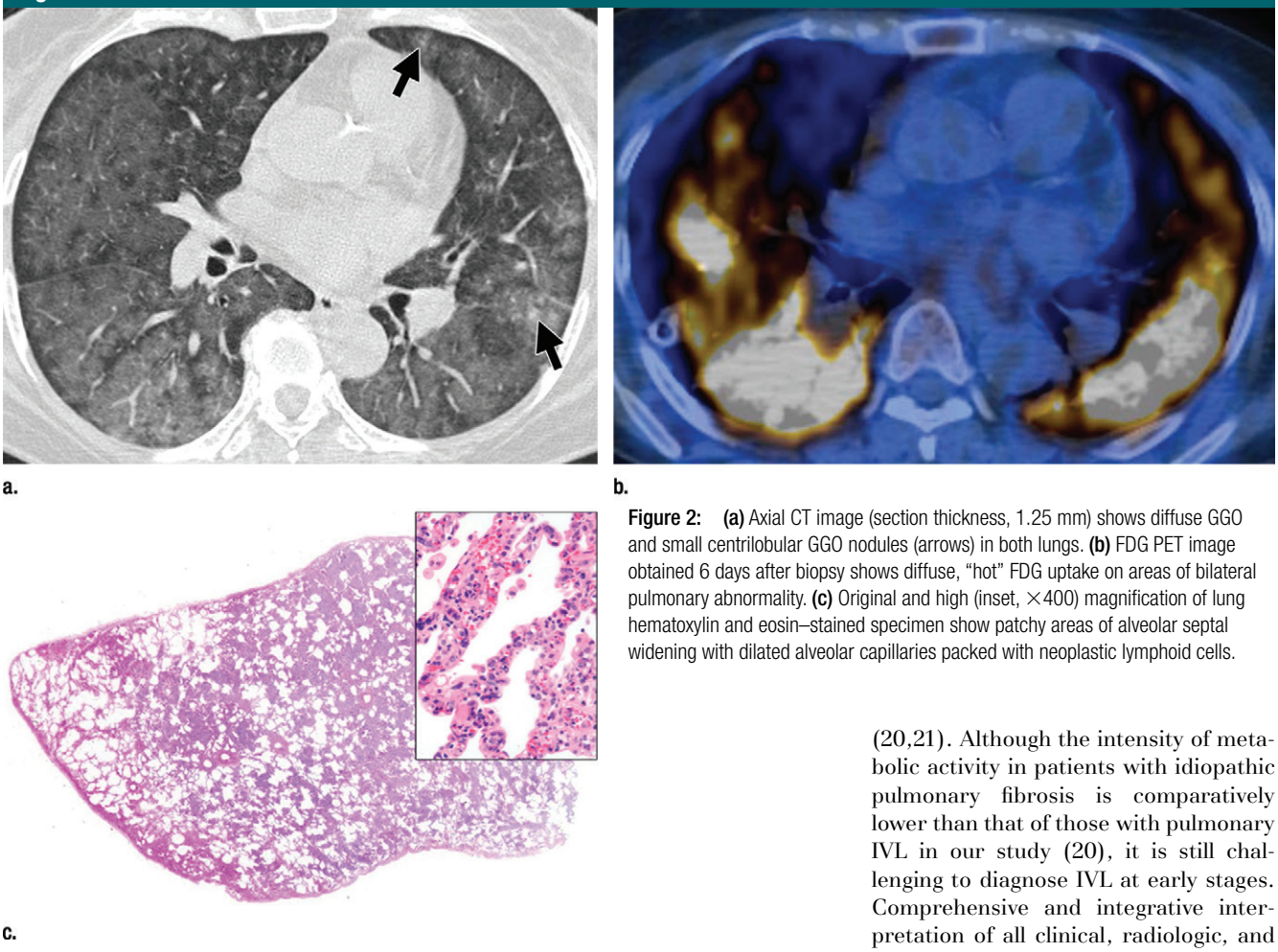

Figure 2: **(a)** Axial CT image (section thickness, 1.25 mm) shows diffuse GGO and small centrilobular GGO nodules (arrows) in both lungs. **(b)** FDG PET image obtained 6 days after biopsy shows diffuse, "hot" FDG uptake on areas of bilateral pulmonary abnormality. **(c)** Original and high (inset, ×400) magnification of lung hematoxylin and eosin–stained specimen show patchy areas of alveolar septal widening with dilated alveolar capillaries packed with neoplastic lymphoid cells.

thickening, and associated lymphadenopathy were not as high as those in the other usual lymphomas (14). These features may support the capillary-, venule-, or arteriole-based dissemination of atypical lymphoid cells in patients with IVL, rather than through lymphatic channels. The parenchymal lesions were predominantly located in the periphery of the lungs in almost half of the patients. This may have been related to vascular occlusion affecting peripheral small vessels rather than large-sized vessels. However, these CT findings are yet nonspecific for IVL, thus detection and identification of other associated radiologic or clinical findings is crucial. For instance, the absence of reticulation, traction bronchiectasis, honeycombing, or architectural distortion on CT images may help to deter us from making a diagnosis of fibrotic interstitial lung disease. Also, CT and echocardiographic features of pulmonary hypertension, noted in five of 11 (46%) patients in our cohort, and decreased diffusion capacity in pulmonary function may become clues for making a correct diagnosis.

Several authors (12,17–19) have reported that FDG PET is useful for diagnosis when IVL is clinically suspected. All patients who underwent FDG PET in our study showed increased FDG uptake in the corresponding lung lesions seen at CT. However, increased pulmonary FDG uptake also can be observed in patients with interstitial lung disease including idiopathic pulmonary fibrosis, which can mimic pulmonary IVL (20,21). Although the intensity of metabolic activity in patients with idiopathic pulmonary fibrosis is comparatively lower than that of those with pulmonary IVL in our study (20), it is still challenging to diagnose IVL at early stages. Comprehensive and integrative interpretation of all clinical, radiologic, and functional imaging findings is essential, and transbronchial lung biopsy should be recommended for the patients who are suspected of having IVL. If it cannot be confirmed with transbronchial lung biopsy, a surgical lung biopsy should be prepared in advance.

Because IVL demonstrates patchy areas of parenchymal opacity, differential diagnoses should include subacute hypersensitivity pneumonitis, atypical pneumonia including *Pneumocystis* pneumonia, diffuse alveolar hemorrhage, and neoplastic conditions. Meticulous acquisition of an environmental and occupational history is important to exclude the possibility of hypersensitivity pneumonitis. In addition, stains and cultures of sputum, blood, or even bronchoalveolar lavage fluid for bacteria and fungi and polymerase

Figure 3

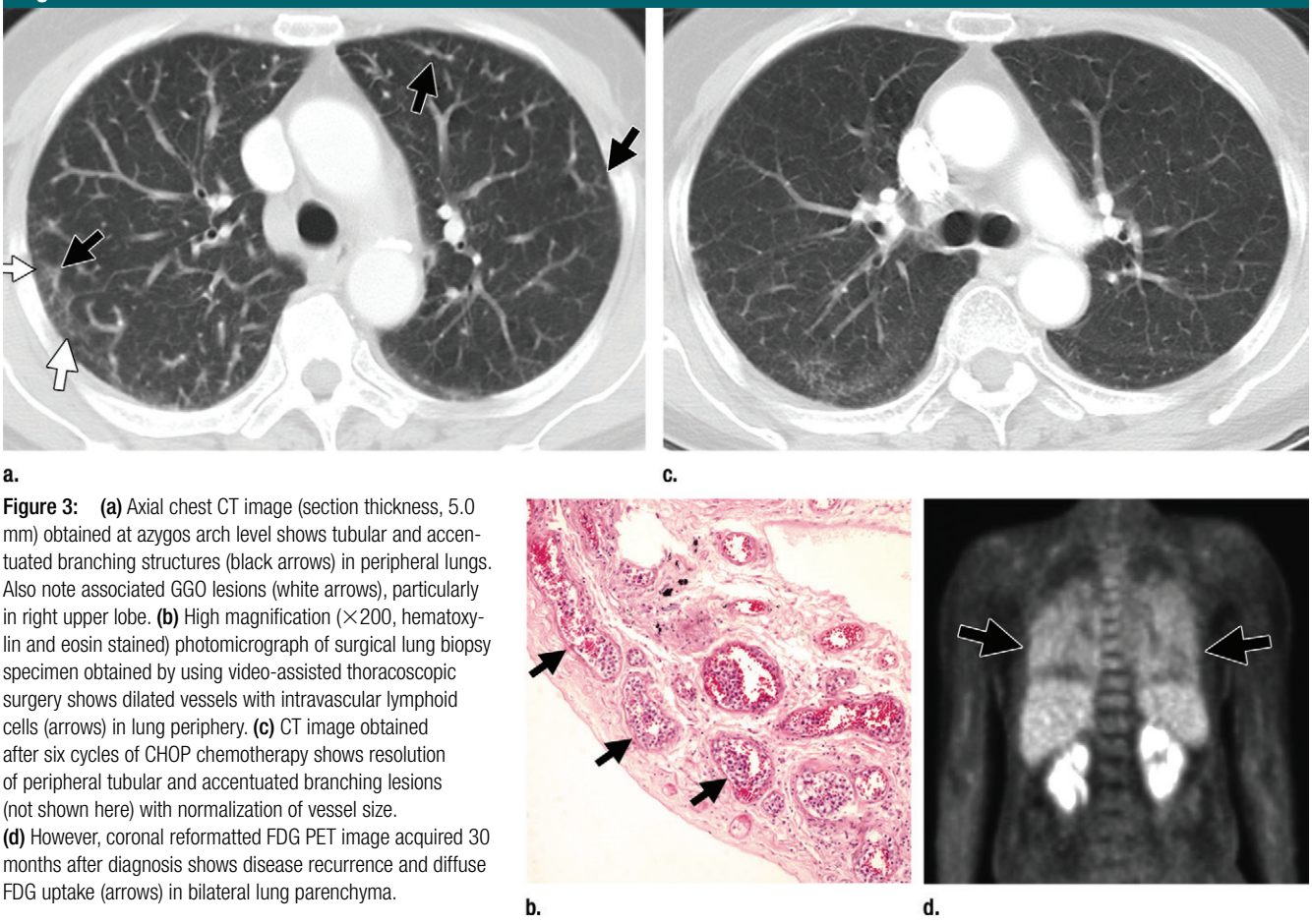

Figure 3: **(a)** Axial chest CT image (section thickness, 5.0 mm) obtained at azygos arch level shows tubular and accentuated branching structures (black arrows) in peripheral lungs. Also note associated GGO lesions (white arrows), particularly in right upper lobe. **(b)** High magnification (×200, hematoxylin and eosin stained) photomicrograph of surgical lung biopsy specimen obtained by using video-assisted thoracoscopic surgery shows dilated vessels with intravascular lymphoid cells (arrows) in lung periphery. **(c)** CT image obtained after six cycles of CHOP chemotherapy shows resolution of peripheral tubular and accentuated branching lesions (not shown here) with normalization of vessel size. **(d)** However, coronal reformatted FDG PET image acquired 30 months after diagnosis shows disease recurrence and diffuse FDG uptake (arrows) in bilateral lung parenchyma.

chain reaction analysis for viral infection should be done for the evaluation of pneumonia. If there is no response to antibiotic or antiviral treatment, the possibility of a neoplastic condition, including pulmonary IVL, should be raised. The neoplastic condition that manifests as diffuse or wide patchy areas of GGO include mucinous or nonmucinous diffuse adenocarcinoma in situ; minimally invasive and invasive adenocarcinoma, secondary involvement of non-Hodgkin lymphoma, particularly T-cell lymphoma; and pulmonary capillary hemangiomatosis (10,22–24). Diffuse nonmucinous and mucinous invasive adenocarcinoma or adenocarcinoma in situ may be seen as diffuse GGO lesions (10,22,23,25). In patients with T-cell lymphoma, lung involvement may appear as bilateral diffuse GGO and interlobular septal thickening (26). The lungs in pulmonary capillary hemangiomatosis may demonstrate bilateral diffuse, centrilobular or lobular, poorly-defined ground-glass nodules with or without interlobular septal thickening at CT. Features of pulmonary hypertension are usually seen in patients with pulmonary capillary hemangiomatosis (27). Because of histologic similarity between pulmonary capillary hemangiomatosis and IVL showing thickened alveolar walls (even though the former is due to capillary proliferation and the latter is due to dilated capillaries with atypical lymphoid cells in alveolar walls), it is hard to distinguish between these two disease entities on the basis of CT. Therefore, we should recommend strongly that histopathologic evaluation, which is mandatory in making a confirmative diagnosis, be conducted.

There were several limitations to our study. First, our study was retrospective in nature and performed in a single institution; thus had a selection bias. Second, we did not perform targeted lung biopsy, thus precise correlation of CT and pathologic results may have been limited. However, we tried to do our best in matching histopathologic results of lung lesions with CT findings at biopsy sites selected on CT images by reviewing surgical reports and by noticing surgical clips identified at follow-up CT performed after the biopsy. Last, the number of patients in the present study was small; thus statistical power, in particular, to detect small differences in survival outcome was limited. To

Table 3

Comparison of Outcomes between Pulmonary and Nonpulmonary IVL

Variable	Pulmonary IVL ($n = 11$)	Nonpulmonary IVL ($n = 31$)	*P* Value
Treatment course			.931
No treatment	0 (0)	3 (10)	
Cessation of treatment	2 (18)	5 (16)	
Ongoing	1 (9)	2 (5)	
Completion	8 (73)	21 (68)	
Regimen of chemotherapy			.086
CHOP	6 (55)	5 (18)	
CHOP with rituximab	5 (45)	22 (79)	
R-Benda	0 (0)	1 (3)	
Survival			.180
Death	7 (64)	12 (39)	
Survival	4 (36)	19 (61)	
Overall survival*	10.8 (0.7–44.8)	18.4 (0.3–119.2)	.338
Length of follow-up*	10.8 (0.7–51.2)	19.0 (0.3–123.5)	
Patients who completed chemotherapy	8	21	
Outcome of chemotherapy			
Death	5 (64)	5 (24)	.083
Survival	3 (36)	16 (76)	
Recurrence	5 (64)	5 (24)	.083
Recurrence free	3 (36)	16 (76)	
Overall survival*	30.0 (8.2–44.8)	31.3 (6.9–119.2)	.110
Recurrence-free survival*	18.9 (4.8–44.8)	31.0 (6.9–119.2)	.065
Length of follow-up*	30.4 (8.2–51.2)	34.5 (8.0–141.4)	

Note.—Unless otherwise indicated, data are number of patients, with percentage in parentheses.

* Data are time in months, with the range in parentheses.

overcome the rarity of pulmonary IVL, we examined the pathologic database of records from a period of 20 years at our institution and finally identified 11 patients in whom the IVL involved the lung parenchyma. A large-scale study based on multicenter data is necessary to identify further the characteristics of this rare malignancy.

In conclusion, the results of our study showed that patients with pulmonary involvement of IVL showed relatively but not significantly poor prognosis compared with those without pulmonary involvement. The most common CT pattern was bilateral GGO with nodules or consolidation. The area of GGO on CT images correlated histopathologically with that of thickened alveolar septa and perivascular spaces because of distended septal capillaries, venules, and arterioles filled with atypical lymphoid cells.

Disclosures of Conflicts of Interest: M.J.C. disclosed no relevant relationships. **K.S.L.** disclosed no relevant relationships. **H.S.H.** disclosed no relevant relationships. **T.J.K.** disclosed no relevant relationships. **T.S.K.** disclosed no relevant relationships. **B.T.K.** disclosed no relevant relationships. **Y.H.K.** disclosed no relevant relationships. **Y.M.S.** disclosed no relevant relationships.

References

1. Yousem SA, Colby TV. Intravascular lymphomatosis presenting in the lung. Cancer 1990;65(2):349–353.
2. DiGiuseppe JA, Nelson WG, Seifter EJ, Boitnott JK, Mann RB. Intravascular lymphomatosis: a clinicopathologic study of 10 cases and assessment of response to chemotherapy. J Clin Oncol 1994;12(12):2573–2579.
3. Ferreri AJ, Campo E, Seymour JF, et al. Intravascular lymphoma: clinical presentation, natural history, management and prognostic factors in a series of 38 cases, with special emphasis on the 'cutaneous variant'. Br J Haematol 2004;127(2):173–183.
4. Murase T, Nakamura S, Kawauchi K, et al. An Asian variant of intravascular large B-cell lymphoma: clinical, pathological and cytogenetic approaches to diffuse large B-cell lymphoma associated with haemophagocytic syndrome. Br J Haematol 2000;111(3):826–834.
5. Ponzoni M, Ferreri AJ, Campo E, et al. Definition, diagnosis, and management of intravascular large B-cell lymphoma: proposals and perspectives from an international consensus meeting. J Clin Oncol 2007;25(21):3168–3173.
6. Demirer T, Dail DH, Aboulafia DM. Four varied cases of intravascular lymphomatosis and a literature review. Cancer 1994;73(6):1738–1745.
7. Treves TA, Gadoth N, Blumen S, Korczyn AD. Intravascular malignant lymphomatosis: a cause of subacute dementia. Dementia 1995;6(5):286–293.
8. Yamagata T, Okamoto Y, Ota K, Katayama N, Tsuda T, Yukawa S. A case of pulmonary intravascular lymphomatosis diagnosed by thoracoscopic lung biopsy. Respiration 2003;70(4):414–418.
9. Jang HJ, Lee KS, Han J. Intravascular lymphomatosis of the lung: radiologic findings. J Comput Assist Tomogr 1998;22(3):427–429.
10. Tokuyasu H, Harada T, Watanabe E, et al. Non-Hodgkin's lymphoma accompanied by pulmonary involvement with diffuse ground-glass opacity on chest CT: a report of 2 cases. Intern Med 2009;48(2):105–109.
11. Cha MJ, Lee HY, Lee KS, et al. Micropapillary and solid subtypes of invasive lung adenocarcinoma: clinical predictors of histopathology and outcome. J Thorac Cardiovasc Surg 2014;147(3):921–928.f.
12. Lee HY, Jeong JY, Lee KS, et al. Solitary pulmonary nodular lung adenocarcinoma: correlation of histopathologic scoring and patient survival with imaging biomarkers. Radiology 2012;264(3):884–893.
13. Hansell DM, Bankier AA, MacMahon H, McLoud TC, Müller NL, Remy J. Fleischner Society: glossary of terms for thoracic imaging. Radiology 2008;246(3):697–722.
14. Hare SS, Souza CA, Bain G, et al. The radiological spectrum of pulmonary lymphoproliferative disease. Br J Radiol 2012;85(1015):848–864.
15. Chong S, Lee KS, Kim TS, Chung MJ, Chung MP, Han J. Adenovirus pneumonia in adults: radiographic and high-resolution CT

findings in five patients. AJR Am J Roentgenol 2006;186(5):1288–1293.

16. Tan RT, Kuzo R, Goodman LR, Siegel R, Haasler GB, Presberg KW. Utility of CT scan evaluation for predicting pulmonary hypertension in patients with parenchymal lung disease. Medical College of Wisconsin Lung Transplant Group. Chest 1998;113(5):1250–1256.

17. Wagner T, Brechemier D, Dugert E, et al. Diffuse pulmonary uptake on FDG-PET with normal CT diagnosed as intravascular large B-cell lymphoma: a case report and a discussion of the causes of diffuse FDG uptake in the lungs. Cancer Imaging 2012;12:7–12.

18. Yamashita H, Suzuki A, Takahashi Y, Kubota K, Kano T, Mimori A. Intravascular large B-cell lymphoma with diffuse FDG uptake in the lung by 18FDG-PET/CT without chest CT findings. Ann Nucl Med 2012;26(6):515–521.

19. Morales-Oyarvide V, Mino-Kenudson M. High-grade lung adenocarcinomas with micropapillary and/or solid patterns: a review. Curr Opin Pulm Med 2014;20(4):317–323.

20. Groves AM, Win T, Screaton NJ, et al. Idiopathic pulmonary fibrosis and diffuse parenchymal lung disease: implications from initial experience with 18F-FDG PET/CT. J Nucl Med 2009;50(4):538–545.

21. Meissner HH, Soo Hoo GW, Khonsary SA, Mandelkern M, Brown CV, Santiago SM. Idiopathic pulmonary fibrosis: evaluation with positron emission tomography. Respiration 2006;73(2):197–202.

22. Okada F, Ando Y, Kondo Y, Matsumoto S, Maeda T, Mori H. Thoracic CT findings of adult T-cell leukemia or lymphoma. AJR Am J Roentgenol 2004;182(3):761–767.

23. Qin L, Shi JH, Liu HR, et al. Non-Hodgkin's lymphoma with diffuse ground-glass opacity on chest CT: a report of 6 cases [in Chinese]. Zhonghua Yi Xue Za Zhi 2010;90(46):3283–3286.

24. El-Gabaly M, Farver CF, Budev MA, Mohammed TL. Pulmonary capillary hemangiomatosis imaging findings and literature update. J Comput Assist Tomogr 2007;31(4):608–610.

25. Akira M, Atagi S, Kawahara M, Iuchi K, Johkoh T. High-resolution CT findings of diffuse bronchioloalveolar carcinoma in 38 patients. AJR Am J Roentgenol 1999;173(6):1623–1629.

26. Watanabe S, Takato H, Waseda Y, et al. Pulmonary T-cell lymphoma with pulmonary arterial hypertension. Intern Med 2011;50(16):1733–1736.

27. Lantuéjoul S, Sheppard MN, Corrin B, Burke MM, Nicholson AG. Pulmonary veno-occlusive disease and pulmonary capillary hemangiomatosis: a clinicopathologic study of 35 cases. Am J Surg Pathol 2006;30(7):850–857.